2022 International Symposium on Nonlinear Theory and Its Applications,
NOLTA2022, Virtual, December 12-15, 2022

A novel hardware efficient wireless walking assist device model and analyses of its various synchronization phenomina

Masaya Kudo† and Hiroyuki Torikai†

†Hosei University, Koganei, Tokyo, Japan
Email: masaya.kudo.9b@stu.hosei.ac.jp, torikai@hosei.ac.jp

Abstract—In this paper, a network of ergodic cellular automaton (CA) oscillators coupled via impulse radio sequences is proposed. The network is implemented by a field programmable gate array and experiments show that the network can exhibit synchronizations with various phase differences. Then, it is discussed that the results of this paper will contribute for developing a wireless walking assist device based on a wireless central pattern generator.

1. Introduction

Recently, a wide variety of walking assist devices have been developed [1][2][3]. For example, Fig.1(a) illustrates the concept of an electrical stimulation device for the treatment of foot drop caused by upper motor neuron injury [2]. The device stimulates muscles of a leg to assist proper walking of a patient. However, if the neuron injury is much more serious, a larger number of muscles should be stimulated properly. For example, to support continuous stationary walking of a patient under serious injury of motor neurons, a large number of muscles of the whole body should be stimulated by rhythmic electric signals with proper phase differences. Note that, in many creatures including humans, such rhythmic signals are believed to be generated by central pattern generators (CPGs) in nervous systems [4]. Then, in this study, we focus on a concept of a future electrical stimulation therapy device based on the CPG as illustrated in Fig.1(b). In order not to disturb the walking of the patient, the nodes (i.e., oscillators) of the CPG should be coupled via wireless signals. Hence, this study designs a network of oscillators coupled via impulse radio sequences [5][6] and analyzes its synchronization phenomena. Note that, compared to our previous study [7], the oscillator in this study is more hardware efficient and the coupling method is more practical.

ORCID iDs First Author: 0000-0001-5397-6742, Second Author: 0000-0003-2795-9628.

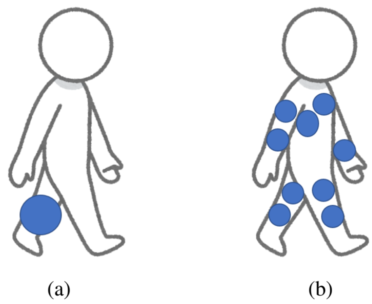

Figure 1: (a) Concept of an electrical stimulation device for the treatment of foot drop caused by upper motor neuron injury [2]. (b) Concept of a future electrical stimulation therapy device based on wireless central pattern generator.

2. Network of Ergodic CA Oscillators Coupled via Impulse Radio Sequences

2.1. Impulse radio sequence

The i-th oscillator of the network is assumed to have its own spreading code $C^{(i)}$, which has the following structure.

$$C^{(i)} = (c_1^{(i)}, c_2^{(i)}, \ldots, c_L^{(i)}),\ \ c_l^{(i)} \in \{0, 1\},$$

where L is the code length and the number K of 1s in the code is assumed to be much smaller than the code length L. Since the code is impulsive and is designed for radio communication mainly, this kind of spreading code is also called an impulse radio sequence [5][6]. Same as the standard code division multiplexing, the impulse radio sequences should have low values of auto-correlation functions (except for zero delay) and cross-correlation functions (for every delay).

2.2. Ergodic CA Oscillator

As the oscillator of the network, the ergodic CA oscillator [8] is employed. The oscillator has four registers, which store discrete state variables X_i and Y_i and discrete auxiliary variables P_i and Q_i defined by

$$\begin{aligned} &X_i \in Z_N = \{0, ..., N-1\}, Y_i \in Z_N, \\ &P_i \in Z_M = \{0, ..., M-1\}, Q_i \in Z_M, \end{aligned} \quad (1)$$

where i is the number of oscillators in the network, $N > 0$ and $M > 0$ are integer parameters, which characterize res-

This work is licensed under a Creative Commons Attribution NonCommercial, No Derivatives 4.0 License.

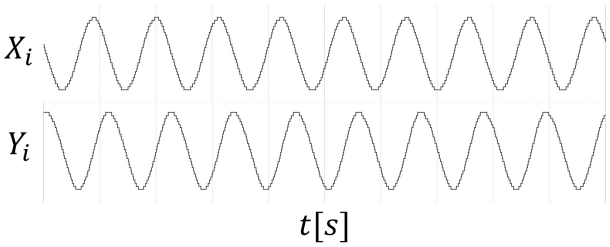

Figure 2: Typical time waveforms of the ergodic CA oscillator. (N, M, α_{xx}, α_{xy}, α_{yx}, α_{yy}, β_x, β_y, ω, T_{Ci}, T_{Xi}, Φ_{Xi}, W_{Xi}, T_{Yi}, Φ_{Yi}, W_{Yi}) = (2^5, 2^6, 1, 1, 1, 1, 2×10^{-5}, $2 \times 10^{-2} T_{Yi}$, $2\pi \times 10^2$, 10^{-3}, 10^{-3}, 0, 10^{-3}, $1.12\sqrt{1.0001} \times 10^{-3}$, 0, 8×10^{-4}).

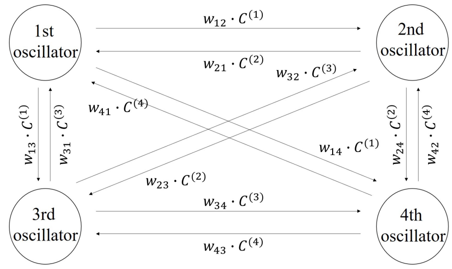

Figure 3: Couple of oscillators via impulse radio sequences. Each i-th oscillator broadcasts its own impulse radio sequence $C^{(i)}$ to all other oscillators when the state Y_i reaches $\lfloor (N-1)/2 \rfloor$ and $X_i > \lfloor (N-1)/2 \rfloor$.

olutions of $\{X_i, Y_i\}$ and $\{P_i, Q_i\}$, respectively, and the variables are saturated at their possible minimum and maximum values. The ergodic CA oscillator receives a periodic clock

$$C_i(t) = \textstyle\sum_{n=0}^{\infty} p(t - nT_{Ci}), \qquad (2)$$

where $p(t)$ is an instantaneous pulse defined by $p(t) = 1$ if $t = 0$, and $p(t) = 0$ if $t \neq 0$; and $T_{Ci} > 0$ is a period of the clock C_i. Furthermore, the oscillator receives two binary switch signals $S_{Xi}(t) \in \{0, 1\}$ and $S_{Yi}(t) \in \{0, 1\}$. In this study, the following periodic switch signals $S_{Xi}(t)$ and $S_{Yi}(t)$ are focused on

$$\begin{aligned} S_{Xi}(t) &= \textstyle\sum_{n=0}^{\infty} q(t - nT_{Xi} - \Phi_{Xi}, W_{Xi}), \\ S_{Yi}(t) &= \textstyle\sum_{n=0}^{\infty} q(t - nT_{Yi} - \Phi_{Yi}, W_{Yi}), \end{aligned} \qquad (3)$$

where $q(t, W)$ is a pulse defined by $q(t) = 1$ if $t \in [0, W]$, and $q(t) = 0$ if $t \notin [0, W]$; $T_{Xi} > 0$ and $T_{Yi} > 0$ are periods; $W_{Xi} \in [0, T_{Xi}]$ and $W_{Yi} \in [0, T_{Yi}]$ are pulse durations; and $\Phi_{Xi} \in [0, T_{Xi})$ and $\Phi_{Yi} \in [0, T_{Yi})$ are initial phases. Then the clock $C_i(t)$ induces the following transitions of the discrete state variables X_i and Y_i.

$$\begin{aligned} &\text{If } C_i(t) = 1, \text{ then} \\ &X_i(t^+) = X_i(t) + S_{Xi}(t)\mathcal{F}_X(X_i(t), Y_i(t), P_i(t)), \\ &Y_i(t^+) = Y_i(t) + S_{Yi}(t)\mathcal{F}_Y(X_i(t), Y_i(t), Q_i(t)). \end{aligned} \qquad (4)$$

where $t^+ = \lim_{\epsilon \to 0} t + \epsilon$ and $\epsilon > 0$; and $\mathcal{F}_X : \mathbf{Z}_N^2 \times \mathbf{Z}_M \to \{-1, 0, 1\}$ and $\mathcal{F}_Y : \mathbf{Z}_N^2 \times \mathbf{Z}_M \to \{-1, 0, 1\}$ are discrete functions, which determine the nonlinear vector field of the oscillator. To use the oscillator as a building block of the CPG, the discrete vector field functions are designed as follows.

$$\mathcal{F}_X(X, Y, P) = \begin{cases} 1 & \text{if } F_X(X, Y) \geq 0 \text{ and } P \geq |F_X(X, Y)|, \\ -1 & \text{if } F_X(X, Y) < 0 \text{ and } P \geq |F_X(X, Y)|, \\ 0 & \text{otherwise,} \end{cases}$$

$$\mathcal{F}_Y(X, Y, Q) = \begin{cases} 1 & \text{if } F_Y(X, Y) \geq 0 \text{ and } Q \geq |F_Y(X, Y)|, \\ -1 & \text{if } F_Y(X, Y) < 0 \text{ and } Q \geq |F_Y(X, Y)|, \\ 0 & \text{otherwise,} \end{cases}$$

where $F_X : \mathbf{Z}_N^2 \to \mathbf{Z}_M^{\pm} = \{-(M-1), -(M-2), \cdots, M-1\}$ and $F_Y : \mathbf{Z}_N^2 \to \mathbf{Z}_M^{\pm}$ are discrete functions given by $F_X(X, Y) = \lfloor (\beta_x f_x(\alpha_{xx}(X - K), \alpha_{xy}(Y - K)))^{-1} \rfloor$, $F_Y(X, Y) = \lfloor (\beta_y f_y(\alpha_{yx}(X - K), \alpha_{yy}(Y - K)))^{-1} \rfloor$, $f_x(x, y) = \delta x - \omega y - x(x^2 + y^2)$, $f_y(x, y) = \omega x + \delta y - y(x^2 + y^2)$, and $K = N/2$; $\lfloor \cdot \rfloor$ is the floor function; F_X and F_Y are saturated at $\pm(M-1)$; α_{xx}, α_{xy}, α_{yx}, α_{yy}, β_x, and β_y are positive parameters for scaling; and $\delta \in \boldsymbol{R}$ and $\omega > 0$ are parameters characterizing the nonlinearity. The discrete auxiliary variables P_i and Q_i work as state-dependent frequency dividers as follows.

$$\begin{aligned} &\text{If } C_i(t) = 1 \text{ and } S_{Xi}(t) = 1, \text{then} \\ &P_i(t^+) = \begin{cases} P_i(t) + 1 & \text{if } \mathcal{F}_X(X_i(t), Y_i(t), P_i(t)) = 0, \\ 0 & \text{otherwise,} \end{cases} \\ &\text{If } C_i(t) = 1 \text{ and } S_{Yi}(t) = 1, \text{then} \\ &Q_i(t^+) = \begin{cases} Q_i(t) + 1 & \text{if } \mathcal{F}_Y(X_i(t), Y_i(t), Q_i(t)) = 0, \\ 0 & \text{otherwise.} \end{cases} \end{aligned} \qquad (5)$$

Fig.2 shows typical time waveforms of the ergodic CA oscillator.

2.3. Coupling via impulse radio sequence

Fig. 3 shows a concept of a network of N ergodic CA oscillators coupled via impulse radio sequences. As shown in the figure, each i-th oscillator broadcasts its own impulse radio sequence $C^{(i)}$ to all other oscillators when the state Y_i reaches $\lfloor (N-1)/2 \rfloor$ and $X_i > \lfloor (N-1)/2 \rfloor$. Then, using an appropriate dispreading circuit, each j-th oscillator ($j \neq i$) can detect the moment when the impulse radio sequence C^i is broadcasted. Based on this detection function, the following coupling method of the oscillators is proposed, where $w_{ij} \in \{-1, 0, 1\}$ is a coupling weight.

Coupling method from i-th oscillator to j-th oscillator: If the j-th oscillaotr receives the impulse radio sequence C^i from the i-th oscillator, $w_{ij} = 1$, and $X_j > \lfloor (N-1)/2 \rfloor$, then the clock period T_j of the j-th oscillator is changed to $T_j + \Delta_j$, where $\Delta_j = k(Y_j - \lfloor (N-1)/2 \rfloor)$ and $k > 0$. If the j-th oscillaotr receives the impulse radio sequence C^i from the i-th oscillator, $w_{ij} = -1$, and $X_j < \lfloor (N-1)/2 \rfloor$, then the clock period T_j of the j-th oscillator is changed to $T_j - \Delta_j$, where $\Delta_j = k(Y_j - \lfloor (N-1)/2 \rfloor)$.

Fig. 4 illustrates the operation of this coupling method.

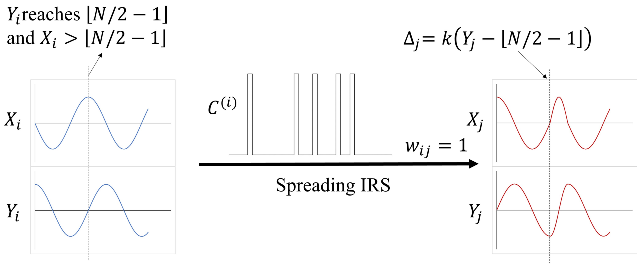

Figure 4: Coupling from the i-th oscillator to the j-th oscillator via the impulse radio sequence $C^{(i)}$.

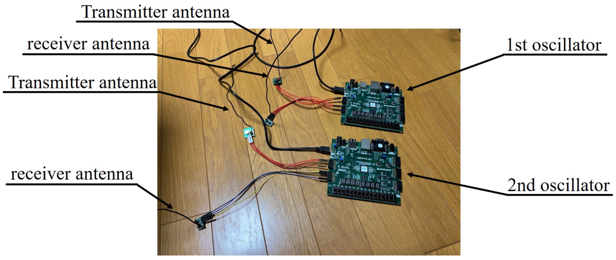

Figure 5: Experimental setup.

3. FPGA Implementation and wireless coupling

In this study, we focused on the following small network.

- The number N of oscillators is 2.
- The 1st and the 2nd oscillators are associated with the impulse radio sequences $C^{(1)}$ and $C^{(2)}$ characterised by

$$\begin{array}{l}(0,0,0,0,1,0,0,0,0,0,0,0,0,0,1,0,0,\\ 0,1,0,0,0,0,1,0,0,1,0,0,0,0,0,0,0,0,0),\\ (0,0,0,0,1,0,0,0,0,0,0,1,0,0,1,0,0,\\ 0,0,0,0,0,0,0,0,0,0,0,1,0,0,0,0,0,1),\end{array} \tag{6}$$

  respectively.
- The physically implemented oscillators are coupled by wireless radio signals.

Under this setting, the network can realize synchronizations by adjusting the coupling weight w_{ij}. The network was implemented by using two field programmable gate array (FPGA) devices (Xilinx's XC7A100T-1CSG324C), where each oscillator was implemented in a single FPGA device as shown in Fig. 5. The two FPGA devices were coupled by radio transmitters and radio receivers as shown in Fig. 5. Figs. 6 shows experimental results. In the case of Fig. 6(a), the coupling weights were set to $w_{12} = w_{21} = 1$ and the oscillators exhibited an in-phase synchronization. In the case of Fig. 6(b), the coupling weights were set to $w_{12} = w_{21} = -1$ and the oscillators exhibited an anti-phase synchronization.

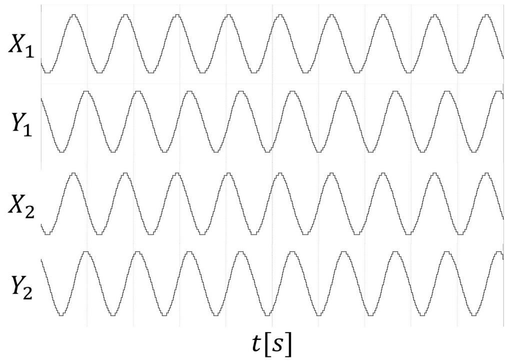

(a)

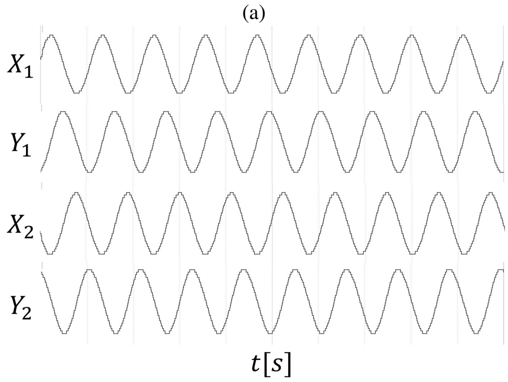

(b)

Figure 6: Oscilloscope snapshots of the proposed network implemented by the FPGAs. The parameter values are the same with those in Fig.2. The clock shift parameter $k = 0.00005$. (a) In-phase synchronization. $w_{12} = w_{21} = 1$. (b) Anti-phase synchronization. $w_{12} = w_{21} = -1$.

4. Discussions and Conclusions

The proposed network of the ergodic CA oscillators coupled via the impulse radio sequences was implemented by the FPGA and radio transmitters and receivers. Experiments showed that the network of two ergodic CA oscillators can realize in-phase and anti-phase synchronizations. We have confirmed that the network size can be extended by using multiple impulse radio sequences and the network can realize various phase differences by extending the proposed coupling method. Hence, the results of this study will contribute for developing a wireless walking assist device based on a wireless central pattern generator. To realize such a wireless walking assist device, we are now investigating the following problems. (a) Implementation of coupled oscillators with other phase differences. (b) Design of a larger network for the wireless walking device. (c) Search of the most appropriate clock shift parameter k.
This work was supported by SCAT and KAKENHI Grant Number 21H03515.

References

[1] K. Takeda, G. Tanino, H. Miyasaka, Review of devices used in neuromuscular electrical stimulation for stroke rehabilitation, Medical Devices: Evidence and Research, vol 10, pp. 207-213, 2017.

[2] https://medical.teijin-pharma.co.jp/zaitaku/product/walkaide/

[3] https://www.og-wellness.jp/product/medical/gd611-612

[4] E. R. Kandel et. al., Principles of Neural Science, Fifth Edition, McGraw-Hill, 2021.

[5] W. Chu and C. J. Colbourn, Sequence designs for ultra-wideband impulse radio with optimal correlation properties, IEEE Trans. Information Theory, vol.50, no.10, pp. 2402-2407, 2004.

[6] T. Iguchi, A. Hirata, and H. Torikai, Theoretical and heuristic synthesis of digital spiking neurons for spike-pattern-division multiplexing, IEICE Tran. Fundamentals, vol. E93-A, no. 8, pp. 1486-1496, 2010.

[7] M. Kudo and H. Torikai, Synchronizations of Hopf Oscillators Coupled via Impulse Radio Sequences: A fundamental research towards designing wireless electrical stimulation therapy device, Proc. of IEEE Workshop on Nonlinear Circuit Networks, pp. 76-78, 2021.

[8] S. Komaki, K. Takeda, H. Torikai, A Novel Ergodic Discrete Difference Equation Model of Central Pattern Generator: Theoretical Analysis and Efficient Implementation, IEEE Trans. Circuits Syst. II, vol. 69, pp. 1767-1771, 2021.